Analysing brilliance spectra of a laser-induced carbon plasma

2006 J. Phys. A: Math. Gen. 39 4731

(http://iopscience.iop.org/0305-4470/39/17/S66)

INSTITUTE OF PHYSICS PUBLISHING JOURNAL OF PHYSICS A: MATHEMATICAL AND GENERAL

J. Phys. A: Math. Gen. **39** (2006) 4731–4737 doi:10.1088/0305-4470/39/17/S66

Analysing brilliance spectra of a laser-induced carbon plasma

B Omar[1], A Wierling[1], S Günter[2] and G Röpke[1]

[1] Universität Rostock, Institut für Physik, 18051 Rostock, Germany
[2] Max-Planck-Institut für Plasmaphysik, 85748 Garching, Germany

E-mail: banaz.omar@uni-rostock.de

Received 28 September 2005, in final form 20 January 2006
Published 7 April 2006
Online at stacks.iop.org/JPhysA/39/4731

Abstract

Brilliance spectra of a carbon plasma generated by subpicosecond high intensity laser pulses are analysed (Wilhein *et al* 1998 *J. Opt. Soc. Am.* **15** 1235). The plasma parameters such as electron density and temperature are determined using a plasma slab model. Synthetic carbon He-α and He-β line profiles are calculated for the inferred plasma parameters by using thermodynamic Green's function, based on a microscopic quantum statistical approach assuming local thermal equilibrium. Self-absorption is taken into account considering one-dimensional radiation transport equation. The comparison between the measured spectrum and our calculated synthetic profile is good for He-α line (C V $1s^2$–1s2p), while discrepancies are found in the case of He-β line (C V $1s^2$–1s3p).

PACS numbers: 44.40.+a, 52.25.Kn, 52.70.−m

(Some figures in this article are in colour only in the electronic version)

1. Introduction

A new area of research in laser-induced plasmas has been opened by using subpicosecond laser pulses to irradiate a solid target. Hot and dense plasmas can be easily created by absorbing laser energy [1, 2] and are a bright source of x-ray radiation [3]. The calculation of spectral He-α and He-β lines are important for the diagnostics of laser-induced plasmas. Recently, a number of high-precision spectroscopic measurements have been carried out by Andiel *et al* [4], Hammel *et al* [5], Beiersdorfer *et al* [6] and Glenzer *et al* [7].

In particular, brilliance measurements of laser-heated plasma with high spectral resolution of laser-heated carbon and boron nitride plasmas have been carried out by Wilhein *et al* [8]. In this experiment, pulses from a KrF laser with an energy of 18 mJ and a duration of 0.7 ps at a wavelength of 248 nm were used. These pulses were focused to a spot with a diameter of 7 ± 3 μm on a polished glassy target. The complete spectrum was generated by averaging

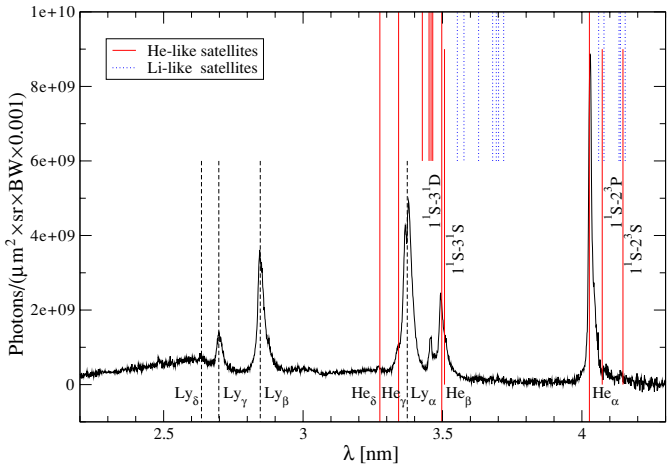

Figure 1. X-ray emission from subpicosecond laser-induced carbon plasma measured at 30° by Wilhein *et al* [8]. Unperturbed positions of H-like, He-like lines, the corresponding satellites and Li-like satellites are also shown by lines at the top of the figure [9].

over 250 shots of laser pulses. The obtained spectrum is shown in figure 1. This spectrum was recorded in the soft x-ray region (2.3–4.4 nm) with high spectral resolution (about 2×10^{-3} nm) at an angle of incidence of 30° . In figure 1, the positions of the unperturbed carbon ion lines and the corresponding satellites lines are depicted [9]. The spectrum is dominated by the emission from C^{5+} and C^{4+} ions, corresponding to H-like Ly-α to Ly-δ and He-like He-α to He-δ lines. Further details of the experimental set-up are given in [8].

In the experiment, the laser pulses couple to the target and generate a hot and dense plasma which undergoes rapid heating and cooling according to hydrodynamic expansion. Clearly, a detailed description of the spectrum emitted by such an expanding plasma in non-equilibrium is a very challenging problem. Often, local thermodynamic equilibrium (LTE) is assumed to use results from advanced line shape calculations for dense plasmas at inferred temperature and density. However, the applicability of such a simplified LTE description has to be justified by estimation from rate equations [10]. In the experiment [8], the transfer code RATION was used to infer the plasma parameters, electron temperature of (80–100) eV/k_B and electron density of $n_e = 4 \times 10^{28}$ m^{-3} by fitting the calculated profile Ly-α with the experimental one, assuming the generated plasma is optically thin.

Recently, the interpretation of the spectra was re-examined by Sorge *et al* [11] using the H-like Lyman lines of the spectrum. Fitting the slope of the Lyman continuum by an exponential Boltzmann expression, a temperature of $T = 86$ eV/k_B was obtained. The electron density $n_e = 3 \times 10^{27}$ m^{-3} was determined from the Stark width, which is very sensitive to n_e, by analysing the H-like Ly-γ line. In order to consider radiation transport, a uniform plasma layer with thickness (30–60) μm was assumed. For these conditions, the synthetic Ly-α and Ly-β spectra match the overall features of the experimental spectra. It has been shown that self-absorption is responsible for strong modifications to the Ly-α as well as Ly-β lines, but less for Ly-γ. The Doppler shift of the Ly-α line due to plasma expansion is about 2.4×10^{-2} nm at the inferred temperature. However, the absorption dip in Ly-α line was not reproduced by Sorge *et al* [11] considering one-layer model only. Therefore, a multi-layer model calculation to reproduce details of the Ly-α line shape is in progress. For this purpose, additional information on the density and temperature conditions are required.

In this communication, we extend our previous study by examining He-like line profiles of the spectrum. Radiation transport is described in the one-dimensional layer model, by assuming local thermal equilibrium, which is characterized by a local electron layer density n_e, temperature T, the streaming of the plasma, and the population of the levels under consideration. The plasma parameters at later time where the He-like ion are predominant, are estimated according to adiabatic expansion starting from the previous values inferred by Sorge *et al* [11] for dominant H-like emitter.

2. Theory

The pressure-broadened line profile is given in quasi-static approximation by averaging the function $L(\omega, \beta)$ over the ionic microfields [11, 12]

$$I^{\mathrm{pr}}(\omega) = \sum_{i,i',f,f'} \frac{\omega^4}{8\pi^3 c^3} \exp\left(-\frac{\hbar\omega}{k_{\mathrm{B}}T}\right) \langle i|\mathbf{r}|f\rangle\langle f'|\mathbf{r}|i'\rangle \times \int_0^\infty \mathrm{d}\beta P(\beta) \mathrm{Im}\langle i|\langle f|L^{-1}(\omega,\beta)|f'\rangle|i'\rangle. \tag{1}$$

Here, the initial and the final atomic states are denoted by i and f, respectively, i' and f' are the corresponding intermediate states [13]. $\langle i|\mathbf{r}|f\rangle$ is the dipole matrix element for the transition between i and f states. The low-frequency microfield distribution function $P(\beta)$ in one-component plasma of carbon ions with effective charge ($Z_i = 4$), is taken according to Potekhin *et al* [14]. The normalized fieldstrength at ion density $n_i = n_e/Z_i$, is given by $\beta = E/E_0$ with the Holtsmark normal field $E_0 = Z_i e/\left(4\pi\epsilon_0 r_0^2\right)$, where $\frac{4}{15}(2\pi)^{3/2} r_0^3 n_i = 1$. The function L is given by

$$L(\omega,\beta) = \hbar\omega - \hbar\omega_{if} - \mathrm{Re}\left[\Sigma_i(\omega,\beta) - \Sigma_f(\omega,\beta)\right] - \mathrm{i}\,\mathrm{Im}\left[\Sigma_i(\omega,\beta) + \Sigma_f(\omega,\beta)\right] + \mathrm{i}\Gamma^{\mathrm{V}}_{if}, \tag{2}$$

where $\hbar\omega_{if} = E_i - E_f$ is the unperturbed line transition frequency and $\Sigma_n(\omega,\beta) = \Sigma_n^{el}(\omega,\beta) + \Sigma_n^{\mathrm{ion}}(\beta)$ is the total self-energy of a state n containing both ionic and electronic contributions to the line shift and width. The difference between the real parts of the initial and final states gives the line shift, while the width arises from adding the initial and final imaginary parts of self-energy.

Starting from a quantum-statistical many-particle approach by using the thermodynamic Green's function technique [15], the electronic self-energies $\Sigma_n^{el}(\omega,\beta)$ for the initial and final states $n = i, f$ and a vertex-correction Γ^V_{if} for the coupling between the initial and final states are derived [11, 12]. This approach generalizes a well-known semiclassical approximation of Griem [13, 16]. In dynamically screened Born approximation [12, 17], the electronic self-energy is determined as

$$\langle n|\Sigma^{\mathrm{el}}\left(E_n^0/\hbar + \delta\omega, \beta\right)|n\rangle = \frac{1}{e^2} - \int \frac{\mathrm{d}^3 q}{(2\pi)^3} V(q) \sum_\alpha \left|M^0_{n\alpha}(\mathbf{q})\right|^2 \times \int_{-\infty}^{\infty} \frac{\mathrm{d}\omega}{\pi}(1 + n_B(\omega)) \frac{\mathrm{Im}\,\varepsilon^{-1}(\mathbf{q},\omega + \mathrm{i}0)}{\hbar\delta\omega - \left(E_\alpha(\beta) - E_n^0\right) - \hbar(\omega + \mathrm{i}0)}. \tag{3}$$

In this expression, $\hbar\delta\omega - \left(E_\alpha(\beta) - E_n^0\right) \approx \left(E_n^0 - E_\alpha^0\right)$ is approximated by the unperturbed transition energy. $n_B(\omega) = \{\exp[\hbar\omega/(k_{\mathrm{B}}T) - 1]\}^{-1}$ is the Bose function, $V(q)$ is the Fourier transform of the Coulomb potential. The dielectric function $\varepsilon(\mathbf{q}, \omega + \mathrm{i}0)$ is taken in random phase approximation [11]. We restricted to neighboured states α, which is taken from $n - 1$ to $n + 1$ discrete bound states for virtual transitions. The transition matrix elements $M_{n\alpha}(\mathbf{q})$

in dipole approximation are evaluated by using the Coulomb approximation method of Bates and Damgaard for the radial wavefunction [18]. The spherical part is approximated by a linear combination of hydrogen-like wave functions.

The static ionic contribution to the ionic self-energy is treated by means of the traditional static microfield concept [13]. The first-order perturbation term vanishes for non-hydrogenic atoms because of nondegeneracy with respect to the orbital quantum number l. The quadratic Stark effect is included according to second-order perturbation theory in the energy. Then, the shift of a level is proportional to the square of the microfield strength [19]

$$\Sigma^2_{nlm}(E) = e^2|E|^2 \left[\frac{|\langle n, l, m|z|n, l+1, m\rangle|^2}{E_{n,l} - E_{n,l+1}} + \frac{|\langle n, l, m|z|n, l+1, m\rangle|^2}{E_{n,l} - E_{n,l-1}} \right], \tag{4}$$

where E is the microfield strength in the z direction, n, l and m are the well-known principal, orbital and magnetic atomic quantum numbers, respectively. The energy difference in the denominator is taken into account for a state differing only in l quantum number. The matrix element $|\langle n, l, m|z|n', l', m'\rangle|$ vanishes except for $l = l' \pm 1$ and $m = m'$. Thus the closest perturbing levels to the level nl are $n, l+1$ and $n, l-1$.

Following Sorge *et al* [11], we use a simple layer model to estimate self-absorption in our exploratory calculations. For a homogeneous layer of density n_e, temperature T, and thickness d, the transfer equation can be solved [20]. The observed intensity $I_{\rm obs}(\omega)$ is given by $I_{\rm obs}(\omega) = (1 - e^{-\tau_\omega})S_\omega(\omega)$, where S_ω is the source function. Assuming local thermodynamic equilibrium, the source function is approximated by the Planck distribution function for black-body radiation [20, 16]. The optical depth of the layer is equal to $\tau_\omega = e^2/(4\epsilon_0 m_e c) f_{fi} n_f I_\omega d$. Here, f_{fi} is the absorption oscillator strength, taken from tables in [21], c is the speed of light and I_ω is the normalized line profile obtained from our quantum statistical approach, see equation (1). n_f is the density of C^{4+} ions in the lower state of the transition. Utilizing both Saha and Boltzmann equations, the density n_f is determined for a given electron density n_e and temperature T. The synthetic profile $I_{\rm obs}(\omega)$ is estimated from the above equation, taking into account the Doppler shift ($\Delta\omega_D = \omega_0 C_s/c$) due to streaming of the expanding plasma, C_s is the ion sound velocity. The electron density is given by $n_e = n_{e0}(d_0/d)$ [2], where n_{e0} is the initial electron density, assumed to be 18×10^{28} m^{-3}, $d_0 \approx 1$ μm the initial thickness, $d = d_0 + C_s t$ is the thickness at time t. The time evolution of the temperature is estimated assuming an adiabatic expansion of the plasma. The mean electron temperature decays in time t according to $T = T_{e0}(d_0/d)^{\gamma-1}$, where $\gamma = 5/3$ is the adiabatic coefficient and T_{e0} is the initial electron temperature, assumed to be 18×10^6 K.

3. Results and discussion

In figures 2 and 3, the comparison between experimental and synthetic spectra for He-α ($1s^2$–1s2p) and He-β ($1s^2$–1s3p) lines are shown, respectively. Two different sets are used: (a) the set inferred by Sorge *et al* [11] for H-like (C VI) with thickness $d = 60$ μm, density $n_e = 3 \times 10^{27}$ m^{-3} and temperature $T = 10^6$ K, and (b) the set determined in this work according to adiabatic expansion with thickness $d = 400$ μm, density $n_e = 4.5 \times 10^{26}$ m^{-3} and temperature $T = 3.32 \times 10^5$ K. The second set and the initial values of the plasma parameters are assumed according to inferred values by Sorge *et al* [11]. Stark broadening is proportional to the electron density. The full width at half maximum for set (a) is 9.617×10^{-4} nm and 8.107×10^{-3} nm for He-α and He-β, respectively, while for set (b), they are 1.365×10^{-4} nm and 1.768×10^{-3} nm . The expansion speed has been estimated from the ion sound velocity $C_s = (Z_i k_{\rm B} T_{e0}/m_i)^{1/2}$, where m_i is the mass of carbon [2]. The Doppler shift of He-α and

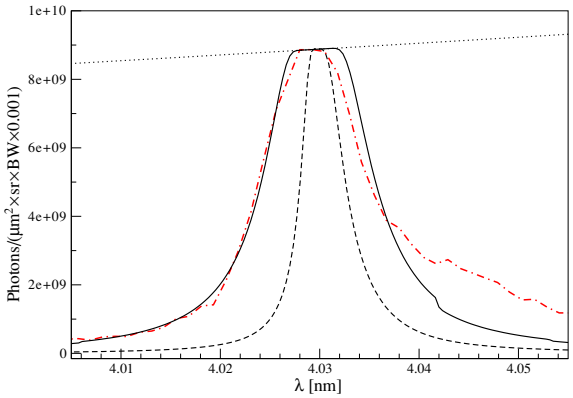

Figure 2. Comparison of the measured He-α profile of carbon target at 30° represented by the dash-dotted line [8] and calculated Stark broadened profiles with the Doppler shift. Self-absorption is included. Two sets of parameters are used. The full line (set (b)) with $n_e = 4.5 \times 10^{26}$ m^{-3}, $T = 3.32 \times 10^5$ K and $d = 400$ μm, the dashed line (set (a)) with $n_e = 3.0 \times 10^{27}$ m^{-3}, $T = 10^6$ K and $d = 60$ μm. The black-body radiation is given by the dotted line.

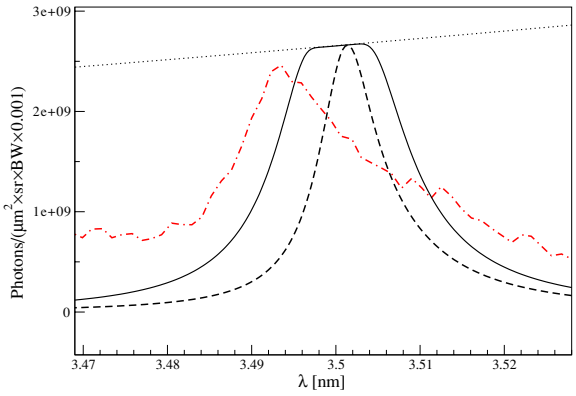

Figure 3. Synthetic He-β profiles represented by the full (set (b)) and the dashed (set (a)) lines for different plasma parameters, see figure 2. Self-absorption is included. Comparison is made with the measured profile (dash-dotted line). The black-body radiation is given by the dotted line.

He-β are 3.3×10^{-3} nm and 2.9×10^{-3} nm, respectively. However, the line broadening of the spectral profile is also related to the thickness and the population of the lower state.

As a result, the total line broadening is larger for set (b) compared to set (a). Besides, the Planck distribution has been fitted to the maximum of the experimental He-α line. Note, that the parameters of Sorge *et al* [11] do not reproduce the experimental results with respect to the He-like ion. This is expected, since plasma conditions of Sorge *et al* [11] refer to a state predominately of C VI ions. After the rapid heating by the laser pulse, the plasma undergoes hydrodynamic expansion. Due to cooling, the carbon ions recombine with free electrons. Assuming local thermodynamic equilibrium, the composition of the plasma is governed by the Saha–Boltzmann equation. Thus, at a later time the He-like emission is expected to dominate the spectrum compared to the H-like emission. The inferred conditions from adiabatic expansion reproduce the experimental spectra to a better extent. The agreement

is quite nice in the line centre and the blue wing of the He-α profile, disagreements exist in the red wing of the profile, where the Li-like satellites appear.

The agreement of the parameter set (b) with the experimental profile is less satisfactory for the He-β line. In addition, the forbidden transitions (1^1 S-3^1 D) and (1^1 S-3^1 S) with $\lambda = 3.499\,53$ nm and $\lambda = 3.507\,31$ nm , respectively, can overlap with the He-β line at $\lambda = 3.497\,28$ nm due to Stark mixing of the wavefunctions at the strong microfield under consideration. The intensity ratios of the corresponding forbidden lines to the allowed one at electron density 4.5×10^{26} m^{-3} are estimated as 0.26 and 0.017, respectively [13, 19]. For this reason, the He-β profile should be performed by taking Stark mixing into account due to forbidden transitions. This will be the subject of future work, as well as the influence of the self-absorption on the line profiles for multi-layer plasma.

Preliminary calculations indicate that the parameter set inferred by Sorge *et al* and the one used here can be linked assuming adiabatic expansion of the plasma [2]. Basing on the plasma conditions of Sorge *et al* [11] the emission time is $t = 0.236$ ns. But the time for the second parameter set corresponds to $t = 1.59$ ns. However, these times have to be put into relation with experimentally measured emission times which are 15 ± 4.5 ps for Ly-β and 32 ± 5 ps for He-α [22]. In order to do so, the expanding plasma with its temperature, density and ionization profiles has to be described in an appropriate manner. It is expected, that these profiles are responsible for the shape of the He-β line as well as for a line inversion of the H-α line [11]. The electron density and temperature gradient in a laser-induced plasma with temporal dynamics is not easy to interpret [23]. Thus, to obtain an appropriate description of the temporal evolution, hydrodynamic codes such as MEDUSA or MULTI have to be used to get these synthetic profiles [23]. The synthetic line profile calculations using such profiles are in progress.

Acknowledgments

This work has been supported by the Deutsche Forschungsgemeinschaft within the Graduiertenkolleg 567 and SFB 652. We would like to thank Professor Hans Griem for valuable discussion.

References

[1] Mancini R C, Shlyaptseva A S, Audebert P, Geindre J P, Bastiani S and Gauthier J C 1996 *Phys. Rev.* E **54** 4147
[2] Theobald W, Hässner R, Wülker C and Sauerbrey R 1996 *Phys. Rev. Lett.* **77** 298
[3] Giulietti D and Gizzi L A 1998 *Riv. Nuovo Cimento* **21** 1
[4] Andiel U, Eidmann K and Witte K 2001 *Phys. Rev.* E **63** 26407
[5] Hammel B A, Keane C J, Cable M D, Kania D R, Kilkenny J D, Lee R W and Pasha R 1993 *Phys. Rev. Lett.* **70** 1263
[6] Beiersdorfer P, Osterheld A L, Phillips T W, Bitter M, Hill K W and von Goeler S 1995 *Phys. Rev.* E **52** 1980
[7] Glenzer S H, Fournier K B, Decker C, Hammel B A, Lee R W, Lours L, MacGowan B J L and Osterheld A L 2000 *Phys. Rev.* E **62** 2728
[8] Wilhein T, Altenbernd D, Teubner U, Förster E, Häßner R, Theobald W and Sauerbrey R 1998 *J. Opt. Soc. Am.* B **15** 1235
[9] Peacock N J, Hobby M G and Galanti M 1973 *J. Phys. B: At. Mol. Opt. Phys.* **6** L298
[10] Leng Y, Goldhar J, Griem H R and Lee R W 1995 *Phys. Rev.* E **52** 4328
[11] Sorge S, Wierling A, Röpke G, Theobald W, Sauerbrey R and Wilhein T 2000 *J. Phys. B: At. Mol. Opt. Phys.* **33** 2983
[12] Günter S and Könies A 1994 *J. Quantum Spectrosc. Radiat. Transfer* **52** 819
[13] Griem H R 1974 *Spectral Line Broadening by Plasmas* (New York: Academic)
[14] Potekhin A Y, Chabrier G and Gilles D 2002 *Phys. Rev.* E **65** 36412

[15] Kraeft W, Kremp D, Ebeling W and Röpke G 1986 *Quantum Statistics of Charged Particle Systems* (Berlin: Akademie Verlag)
[16] Griem H R 1997 *Principles of Plasma Spectroscopy* (Cambridge: Cambridge University Press)
[17] Günter S, Hitzschke L and Röpke G 1991 *Phys. Rev.* A **44** 6834
[18] Bates D R and Damgaard A 1949 *Phil. Trans. R. Soc. Lond.* A **242** 101
[19] Bethe H A and Salpeter E E 1977 *Quantum Mechanics of One- and Two-Electron Atoms* (New York: Plenum)
[20] Rybicki G G and Lightman A P 1979 *Radiative Processes in Astrophysics* (New York: Wiley)
[21] Verner D A, Vernaer E M and Terland G J 1996 *At. Data Tables* **641**
[22] Wülker C, Theobald W and Schäfer F P 1994 *Phys. Rev* E **50** 4920
[23] Audebert P, Shepherd R, Fournier K B, Peyrusse O, Price D, Lee R W, Springer P, Gauthier J-C and Klein L 2002 *Phys. Rev.* E **66** 66412